J. Appl. Math. & Informatics Vol. **29***(2011), No. 1 - 2, pp. 427 - 442*
Website: http://www.kcam.biz

FINITE ELEMENT MODEL TO STUDY TWO DIMENSIONAL UNSTEADY STATE CYTOSOLIC CALCIUM DIFFUSION

SHIVENDRA G. TEWARI* AND K.R. PARDASANI

Abstract. Calcium is a vital second messenger for signal transduction in neurons. Calcium plays an important role in almost every part of the human body but in neuronal cytosol, it is of utmost importance. In order to understand the calcium signaling mechanism in a better way a finite element model has been developed to study the flow of calcium in two dimensions with time. This model assumes EBA (Excess Buffering Approximation), incorporating all the important parameters like time, association rate, influx, buffer concentration, diffusion constant etc. Finite element method is used to obtain calcium concentration in two dimensions and numerical integration is used to compute effect of time over 2-D Calcium profile. Comparative study of calcium signaling in two dimensions with time is done with other important physiological parameters. A MATLAB program has been developed for the entire problem and simulated on an x64 machine to compute the numerical results.

AMS Mathematics Subject Classification : 65N30, 92B99.
Key words and phrases : Association rate, EBA, Diffusion constant, Influx, Calcium profile.

1. Introduction

Communication in neurons is done through two synapses 1) Electrical synapse and 2) Chemical synapse. The signaling done through electrical synapse is fast while the signaling through chemical synapse is slow. Even though, the signaling through chemical synapses is more significant than electrical synapses as it comes into play when the distance between the neurons is more than 4-5 nm [5]. When the distance in between neurons is more, then signaling in between neurons cannot be done through electrical synapses. In this case, electrical signal is converted into a chemical one so that signal can be transmitted through the chemical synapse. This process of conversion of an electrical signal into a

Received September 27, 2009. Revised November 19, 2009. Accepted November 13, 2010.
*Corresponding author.
© 2011 Korean SIGCAM and KSCAM.

chemical signal is known as the process of signal transduction. Calcium is an important switch that decides whether a particular electrical signal is to be converted into a chemical signal or not. This Ca^{2+} is known to regulate a number of cellular functions like synaptic plasticity, gene expression, muscle contraction etc. [9], calcium is also known as an important second messenger. When an electrical signal arrives near the end point of an axon (cytosol), it causes the Voltage Dependent Calcium Channels (VDCC) to open which facilitates the inflow of extracellular Ca^{2+} inside the cytosol. This inflow of Ca^{2+} creates transient domains of high intracellular Ca^{2+} concentration near the *VDCC* [11]. Near these *VDCC*'s there are synaptic vesicles which contain neurotransmitters and here $[Ca^{2+}]_i$ attaches with *synaptotagmin* (an integral protein of synaptic vesicle) to initiate the process of exocytosis [2]. Since, exocytosis occurs in the immediate vicinity of *VDCC*'s therefore, $[Ca^{2+}]_i$ transient cannot be directly measured due to the spatiotemporal limitations of the $[Ca^{2+}]_i$ measuring technologies [14]. Mathematical and Computational simulation of Ca^{2+} kinetics provides an important alternative to study the effect of several parameters over $[Ca^{2+}]_i$ transients [7,11,12]. In this paper, the Ca^{2+} dynamics are studied by developing a two dimensional Finite Element Model for unsteady state Ca^{2+} diffusion in neurons. A computer program has been developed in MATLAB for the whole approach and simulated on an AMD Turion 64x2 machine with 1.6 GHz processing speed and 2.5 GB memory. The numerical results are used to display the two-dimensional Ca^{2+} profile in x and y directions. Also, the numerical results are used to study the relationships between Ca^{2+}, diffusion constant, buffer concentration, association rate etc.

2. Mathematical Formulation

Calcium kinetics in neurons is governed by a set of reaction-diffusion equations which can be framed assuming the following bimolecular reaction between Ca^{2+} and buffer species,

$$[Ca^{2+}] + [B_j] \underset{k^-}{\overset{k^+}{\rightleftharpoons}} [CaB_j] \tag{1}$$

where $[B_j]$ and $[CaB_j]$ are free and bound buffer respectively, and 'j' is an index over buffer species. Thus, Calcium dynamics can be framed in the form of following equations [7,11,12]:

$$\frac{\partial [Ca^{2+}]}{\partial t} = D_{Ca}\left(\frac{\partial^2 [Ca^{2+}]}{\partial x^2} + \frac{\partial^2 [Ca^{2+}]}{\partial y^2}\right) + \sum_j R_j + \sigma\delta(r) \tag{2}$$

$$\frac{\partial [B_j]}{\partial t} = D_{B_j}\left(\frac{\partial^2 [B_j]}{\partial x^2} + \frac{\partial^2 [B_j]}{\partial y^2}\right) + R_j \tag{3}$$

$$\frac{\partial [CaB_j]}{\partial t} = D_{CaB_j}\left(\frac{\partial^2 [CaB_j]}{\partial x^2} + \frac{\partial^2 [CaB_j]}{\partial y^2}\right) - R_j \tag{4}$$

where,

$$R_j = -k_j^+[B_j][Ca^{2+}] + k_j^-[CaB_j] \tag{5}$$

D_{Ca}, D_{B_j}, D_{CaBj} are diffusion coefficient of free calcium, free buffer, and Ca^{2+} bound buffer, respectively; $\delta(r)$ is the well known dirac delta function operating at the Ca^{2+} source; k_j^+ and k_j^- are association and dissociation rate constants for buffer 'j', respectively. For stationary, immobile buffers or fixed buffers $D_{B_j} = D_{CaB_j} = 0$. The first term on the right hand side of (2) comes as a result of Fick's law of diffusion, the second term R_j is known as the reaction diffusion term and the third term is the source amplitude due to the calcium channel. If we assume a single mobile buffer species, i.e. $[B_j] = [B]$ and assume two things 1) Excess Buffer Approximation (EBA), due to Neher [7], i.e. the buffer concentration is present in excess and 2) Buffer is constant in space and time, i.e. $[B] = [CaB]$ = constant, then (2)-(5) can be simplified to,

$$\frac{\partial[Ca^{2+}]}{\partial t} = D_{Ca}\left(\frac{\partial^2[Ca^{2+}]}{\partial x^2} + \frac{\partial^2[Ca^{2+}]}{\partial y^2}\right) - k_m^+[B]_\infty\left([Ca^{2+}] - [Ca]_\infty\right) + \sigma\delta(r) \tag{6}$$

where, $[B]_\infty$ and $[Ca]_\infty$ are steady state buffer and calcium concentration respectively. In this paper, we have considered cytosol to be a circle of radius 5 μm. The centre of the circle is supposed to be situated at origin (i.e. *x = 0, y = 0*). We have assumed that there is a point source of calcium situated at *x = -5, y = 0*. An appropriate flux condition for it can be framed as [11,12]:

$$\lim_{x\to -5, y\to 0} -D_{Ca}\frac{d[Ca^{2+}]}{dx} = \sigma \tag{7}$$

For boundary and initial conditions, it is assumed that $[Ca^{2+}]$ attains its background concentration of 0.1 μM as it goes far away from the source i.e.

$$\lim_{x\to 5, y\to 0}[Ca^{2+}] = [Ca]_\infty \tag{8}$$

And initially, the cytosolic $[Ca^{2+}]$ concentration is 0.1 μM. Further, the cytosol is divided into 60 linear triangular elements of different sizes (see Figure 1). The discretized variational form of (6)-(8) can be written as,

$$I^{(e)} = \frac{1}{2}\int\int_A \left\{\left(\frac{du^{(e)}}{dx}\right)^2 + \left(\frac{du^{(e)}}{dy}\right)^2 + \frac{u^{(e)2}}{\lambda^2} - \frac{2u^{(e)}u_\infty}{\lambda^2} + \frac{2u^{(e)}}{D_{Ca}}\frac{\partial u^{(e)}}{\partial t}\right\} dA$$
$$-\mu^{(e)}\int_{y_i}^{y_j}\left(\frac{\sigma}{D_{Ca}}\, u^{(e)}\Big|_{x=-5}\right) dy \tag{9}$$

Here, we have used 'u' in lieu of $[Ca^{2+}]$ for our convenience, e = 1,2,...,60, λ is the characteristic length and is equal to $\sqrt{D_{Ca}/k_m^+[B]_\infty}$. Also the second term ($\mu_{(e)} = 1$) for e = 30,33 and ($\mu_{(e)}$=0) for rest of the elements. The shape function of concentration variation within each element is defined by [8]:

$$u^{(e)}(x,y) = N_i^{(e)}(x,y)u_i^{(e)} + N_j^{(e)}(x,y)u_j^{(e)} + N_k^{(e)}(x,y)u_k^{(e)} \tag{10}$$

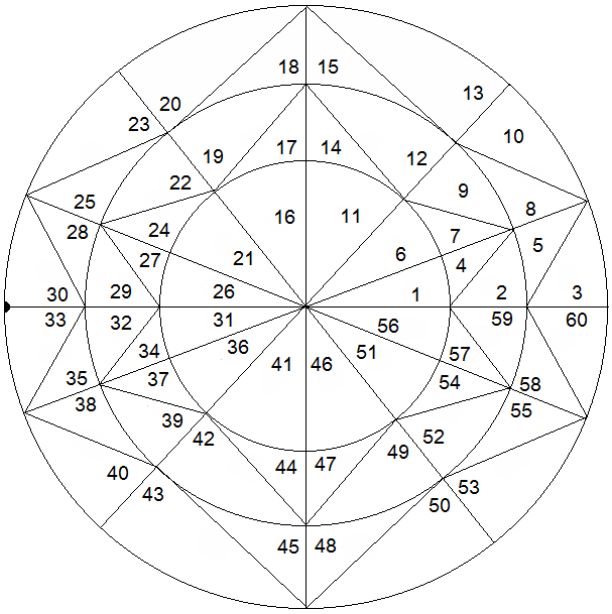

FIGURE 1. Finite Element discretization of the cytosol, small black circle at interface of element numbers '30' and '33' represents point source of calcium.

where, u_i, u_j, u_k are nodal Ca^{2+} concentrations and N_i, N_j and N_k are element shape functions given by,

$$\begin{aligned} N_i^{(e)}(x,y) &= \tfrac{1}{2A^{(e)}}(a_i^{(e)} + b_i^{(e)}x + c_i^{(e)}y) \\ N_j^{(e)}(x,y) &= \tfrac{1}{2A^{(e)}}(a_j^{(e)} + b_j^{(e)}x + c_j^{(e)}y) \\ N_k^{(e)}(x,y) &= \tfrac{1}{2A^{(e)}}(a_k^{(e)} + b_k^{(e)}x + c_k^{(e)}y) \end{aligned} \tag{11}$$

Here, $A^{(e)}$ is the area of each element and a_i, a_j, a_k, b_i, b_j, b_k, c_i, c_j and c_k are:

$$\begin{aligned} a_i &= x_j y_k - x_k y_j \\ a_j &= x_k y_i - x_i y_k \\ a_k &= x_i y_j - x_j y_i \\ b_i &= y_j - y_k \\ b_j &= y_k - y_i \\ b_k &= y_i - y_j \\ c_i &= x_k - x_j \\ c_j &= x_i - x_k \\ c_k &= x_j - x_i \end{aligned} \tag{12}$$

Now, using (10)-(12) in (9) and extremizing (9) with respect to nodal concentrations we have,

$$\frac{\partial I^{(e)}}{\partial u_i} = \int\int_A \left(\frac{\partial N^{(e)}}{\partial x}\frac{\partial {N^{(e)}}^T}{\partial x} + \frac{\partial N^{(e)}}{\partial y}\frac{\partial {N^{(e)}}^T}{\partial y} \right) u^{(e)} dA$$
$$+ \int\int_A \frac{1}{\lambda^2}(N^{(e)}{N^{(e)}}^T)u^{(e)}dA + \int\int_A \frac{1}{D_{Ca}} N^{(e)}{N^{(e)}}^T \frac{\partial u^{(e)}}{\partial t} dA$$
$$- \int\int_A \frac{N^{(e)}u_\infty}{\lambda^2} dA - \mu^{(e)} \int_{y_i}^{y_j} \frac{\sigma}{D_{Ca}} N^{(e)} \Big|_{x=-5} dy \qquad (13)$$

Here, $u^{(e)} = \begin{bmatrix} u_i & u_j & u_k \end{bmatrix}^T$. Assembling (13) for e = 1,2,...,60, we have,

$$\frac{\partial I}{\partial u_i} = \sum_{e=1}^{60} \frac{\partial I^{(e)}}{\partial u_i} = 0 \qquad (14)$$

where, i = 1,2,..., 37. Rearranging (14) and writing in matrix form, we have a system of ordinary differential equations (see Appendix for details),

$$[K]_{37x37}\,[\overline{u}]_{37x1} + [M]_{37x37}\left[\frac{\partial \overline{u}}{\partial t}\right]_{37x1} = [F]_{37x1} \qquad (15)$$

here, $\overline{u}$= u_1, u_2, ..., u_{37}, K and M are system matrices, and F is the system vector. For the solution of (15), we have developed a computer program in MATLAB that uses numerical integration to approximate the solution at discrete time steps [6]. The time taken for simulation (rate 1 Hz) is nearly 2 minutes on an AMD Turion 64x2 machine with 1.6 GHz processing speed and 2.5 GB memory.

3. Results and Discussion

In this section, numerical results are shown in the form of figures explaining the relationship observed between the physiological parameters. The parameters used are as stated in Table 1 until unless stated with the figure [1,11,13]:
In Figure 2, the cytosolic diffusion is shown in two directions, namely x and y directions, for time t = 100 ms. As proposed Ca^{2+} attains its background concentration of 0.1 μM as it goes far away from the Ca^{2+} channel. Since the source amplitude is taken to be only 1 pA therefore the highest Ca^{2+} concentration observed is only 1.762 μM. Thus, if a signal arrives at the mouth of channel which causes depolarization of the membrane and leads to the opening of VDCC's, can only increase the intracellular Ca^{2+} concentration to an extent of 1.762 μM. As observed by Brose *et al.* [3], synaptotagmin is activated only at high cytosolic $[Ca^{2+}]\sim 10\mu M$ and not at low concentrations $[Ca^{2}]\sim 1\mu M$. Thus, no signal transduction is supposed to take place at this point of time.

In Figure 3, we have shown the variation in $[Ca^{2+}]$ along the x-axis. This is as if we are studying diffusion in only one dimension. As expected, cytosolic $[Ca^{2+}]$ is highest at the source and it starts decaying as it diffuses along the x-axis. This is to show that there is no change in the way $[Ca^{2+}]$ diffuses in x-axis

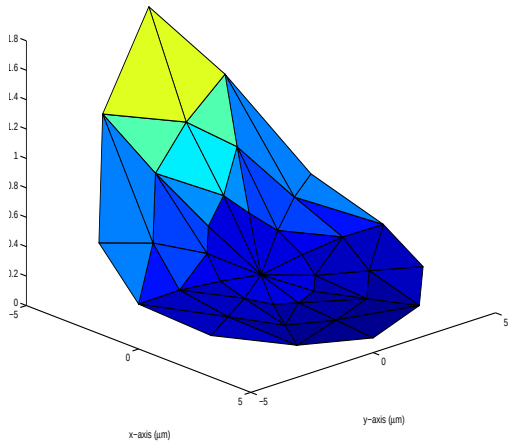

FIGURE 2. Calcium profile showing its diffusion in x and y directions for time, t = 100 ms. In this figure and the figures to follow source amplitude is converted into μM / sec by using Faradays constant and using the fact that 1 L = $10^{15}\mu m$.

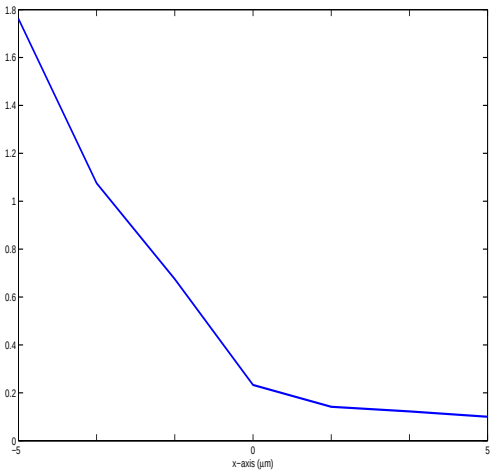

FIGURE 3. Figure showing diffusion of $[Ca^{2+}]$ along x-axis alone.

Symbol	**Parameter**	**Value**
D_{Ca}	Diffusion coefficient	250 μm^2 / second
k_m^+(EGTA)	Buffer association rate	1.5 $\mu M^{-1} second^{-1}$
k_m^+(BAPTA)	Buffer association rate	600 $\mu M^{-1} second^{-1}$
$[B_m]_\infty$	Buffer concentration	50 μM
$[Ca^{2+}]_\infty$	Background Ca^{2+} Concentration	0.1 μM
σ	Source amplitude	1 pA
F	Faraday's Constant	96487 Coulombs/moles
V	Volume of the cytosol	523.6 μm^3

TABLE 1. List of physiological parameters used for computing numerical results[1,11,12,13]

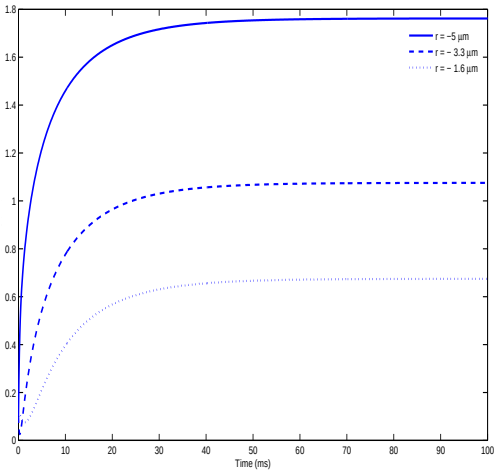

FIGURE 4. Figure showing variation in nodal concentrations along x-axis with respect to time.

because of the introduction of y-axis. Therefore, all the hypothesis proposed by previous researchers for one dimension also hold here. This also validates our mathematical model.

In Figure 4, we have shown the variation in $[Ca^{2+}]$ concentration with respect to time. The variations are shown for three different positions first one is at source(thick continuous line) i.e. at the place of *VDCC*, the second one is at a distance 1.6 μm away from the source(broken line) and the third one is at a distance 3.3 μm from the source(thin continuous line). It is apparent from

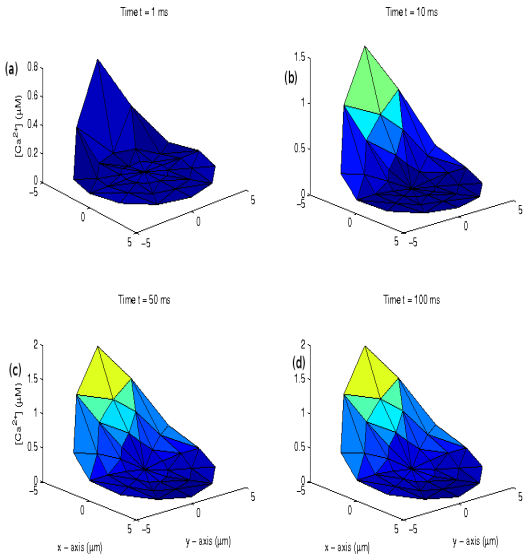

FIGURE 5. Figure showing the effect of increasing time over two dimensional calcium profile.

the figure that $[Ca^{2+}]$ concentration rises for sometime but as it reaches steady state concentration it tends to relax and settles to the steady state concentration. These results are also in agreement with previous researchers. The results shown here are only for variation along x-axis, in the next figure same thing has been shown in two dimensions i.e. x and y directions.

In figure 5, the effect of time over two-dimensional calcium profile is shown. This figure is in continuation with the previous figure except for the fact that here changes with respect to time are observed for whole of the cytosol. It is apparent from the figure that calcium begins to rise slowly as time elapses and attains a steady state calcium concentration of 1.76 μM. It was also observed that there is no change in calcium profile after 100 ms (not shown in this paper) which means that calcium attains steady state after 100 ms.

In figure 6, the changes in calcium concentration is shown for two different pathways. First one(broken line) shows the decay in calcium concentration if we proceed along the circumference to the end point (i.e. $x = 5$, $y = 0$). Second one(continuous line) is the same plot as figure 3, i.e. along the x-axis. In this figure, the differences in decay have been shown. The first one decays faster than the second one for 'x' belonging to the interval [-5, 0], it is because of the fact that we are going away from the source in both the directions (x and y axes) but both the graphs decay nearly at the same rate as we enter inside the interval [0, 5]. The second one decays at a constant rate throughout the interval [-5, 5].

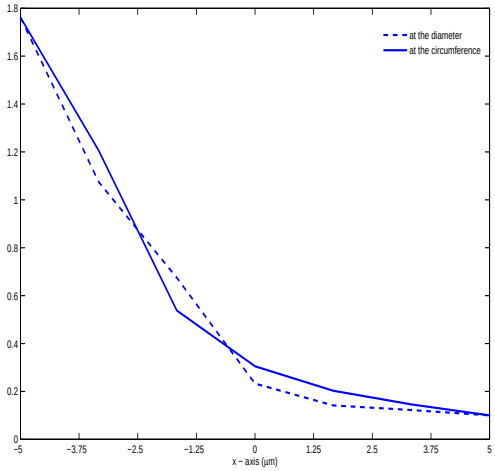

FIGURE 6. Figure showing the decay in calcium concentration via two different paths.

It was necessary to study the behavior of calcium decay at the circumference because it will be helpful for researchers who are trying to incorporate a calcium induced calcium channel in the mathematical model of cytosolic calcium diffusion. With the help of this variation they can decide where to place the site of calcium induced calcium channel, so that it can be initialized.

In figure 7, there are two curves showing calcium diffusion. First one(continuous line), in the figure is when $\theta = 0^\circ$ i.e. when y = 0 (x-axis). The second curve(broken line) is for $\theta = 30^\circ$, it was observed (not shown in this paper) and is obvious that whether we change the angle with respect to x-axis clockwise or anticlockwise the second curve is same. The first curve is same as figure 3, as we are talking about diffusion along x-axis. In the second curve, the maximum calcium concentration observed is 1.2 μM because we are away from the source. Likewise, the decay is also slow because it is away from the constrained node. In both the curves, the source was at the same place i.e. x = -5, y = 0.

In figure 8, there are three curves shown, basically they are special cases of figure 6, where we are talking about diffusion of calcium at different distances from the source measured along x-axis namely, 1) at the source, 2) at a distance 1.6 μm from source (i.e. x = -3.3 μm) and 3) at a distance 3.3 μm from the source. It is apparent from the figure that there is a significant change in the way calcium diffuses and also in the magnitude of calcium concentration. Also, it is clear from the figure that calcium concentration is decreasing as we are going away from the calcium source. So whatever synaptic vesicles that are there in the cytosol would have to be very near to the channel in order to release the

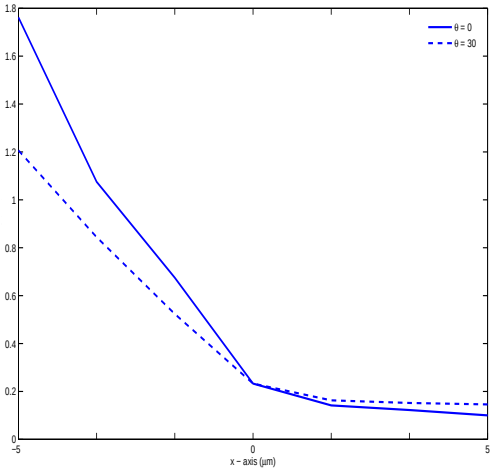

FIGURE 7. Showing the change in diffusion of calcium when we alter the angle at which diffusion takes place keeping the source of calcium as constant.

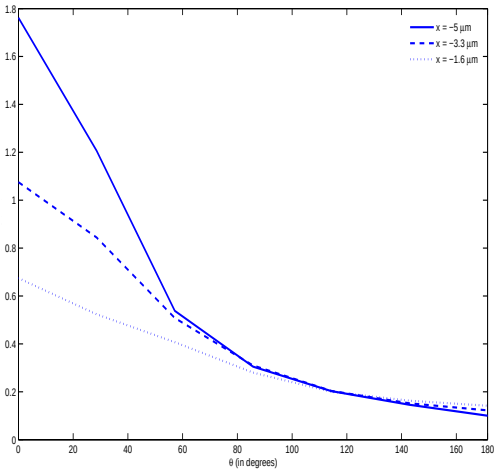

FIGURE 8. Figure showing changes in calcium diffusivity with respect to the circumference for different distances from the calcium channel.

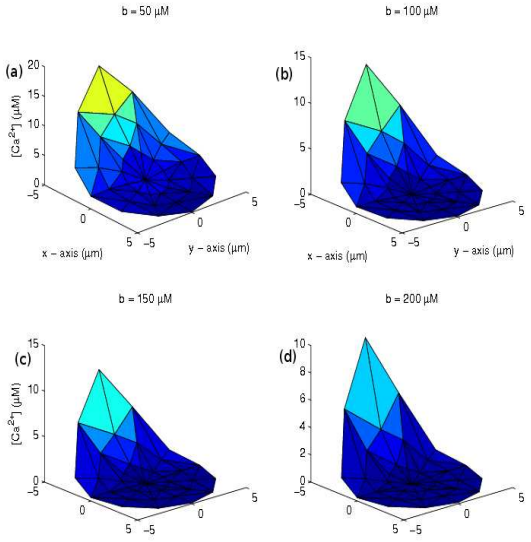

FIGURE 9. Figure showing the effects of increasing buffer concentration on two dimensional calcium profile for source amplitude σ=10 pA.

transmitters. Statistically, at least three calcium ions must bind to a synaptic vesicle for neurotransmitters to be released [4].

Figure 9 showing the effect of increasing buffer concentration for time t = 100 ms, (a) is for buffer concentration taken to be 50 μM, (b) is for buffer concentration taken to be 100 μM, (c) is for buffer concentration taken to be 150 μM, and (d) is for buffer concentration taken to be 200 μM. In all the three cases we are talking about the concentration of *Ethylene Glycol-bis (beta-aminoethyl-ether)-N,N,N',N'-TetraAcetate* (EGTA). As expected the increase in buffer concentration increases the decay of calcium which is evident in both the directions. In other words, it can be said that increase in buffer concentration alters the time required to achieve the steady state.

Figure 10 shows changes in the cytosolic calcium profile for increasing source amplitude σ. As shown from the figure the relationship between calcium concentration and source amplitude is nearly linear. This thing is evident from the figure as source amplitude is increasing, the peak of calcium concentration is also getting higher. This fact was also observed by Smith [11] that as source amplitude is increased the relationship between calcium and source amplitude becomes linear, but the studies done by Smith [11] were for Rapid buffering Approximation (RBA). In fact, if we plot the graph between the calcium and source amplitude it will be a linear graph (not shown in this paper).

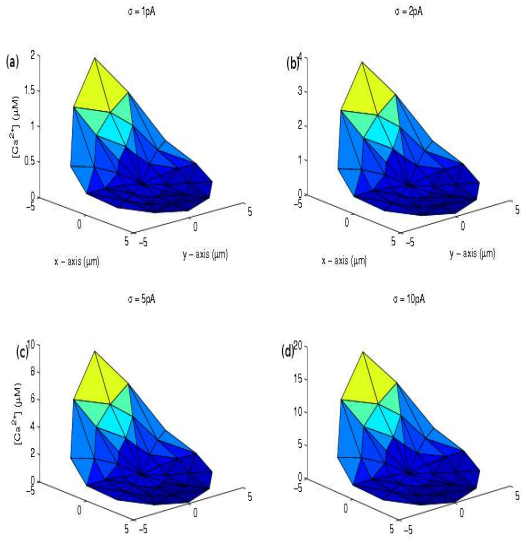

FIGURE 10. Figure showing changes in cytosolic calcium due to an increase in source amplitude at time,t=100ms.

In figure 11, the effect of different calcium chelators on cytosolic calcium profile is shown. These chelators are used to increase or decrease the time required by calcium to attain steady state. We used two exogenous buffers 1) BAPTA (*1,2-bis(o-minophenoxy)ethane-N,N,N',N'-tetraacetic acid*) which is a very fast calcium chelator 2) EGTA which is a slow chelator. Figure 11(a) is for EGTA and 11(b) is for BAPTA, as expected when we introduce BAPTA inside the cytosol instead of EGTA it binds very rapidly to calcium and reduces the free calcium concentration. It is evident from the figure that the highest calcium concentration in 11(b) is only 1 μM while the same for 11(a) is nearly 20μM.
The results obtained in this paper are in agreement with the physiological facts. Some of the results obtained have also been observed by previous researchers but they were all for one – dimensional case. Whatever new results that are obtained in this paper are also in agreement with the physiological facts. The results obtained in this paper can be very useful for researchers to develop more detailed mathematical model to have a more realistic cytosolic environment. The results are about the changes in cytosolic calcium diffusion with respect to different parameters, which give us information about the relative effect of each parameter over cytosolic calcium diffusion. Further, the results obtained can be of great use to biomedical scientists for development of new protocols for treatment and diagnosis of neuronal diseases.

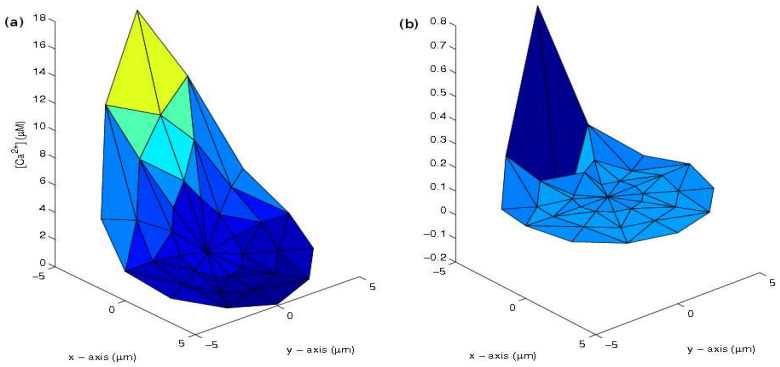

FIGURE 11. All the parameter are same as stated in Table 1 except for , time t = 100 ms and buffer type. Figure showing change in calcium profile for different calcium chelators namely BAPTA and EGTA.

Acknowledgement

The authors are highly grateful to Department of Biotechnology, New Delhi, India for providing support in the form of Bioinformatics Infrastructure Facility for carrying out this work.

Appendix

When we extremize (9) we have,

$$\begin{aligned}\frac{\partial I^{(e)}}{\partial u_i} = \iint_A \left(\frac{\partial u^{(e)}}{\partial x} \frac{\partial}{\partial u_i} \left(\frac{\partial u^{(e)}}{\partial x} \right) + \frac{\partial u^{(e)}}{\partial y} \frac{\partial}{\partial u_i} \left(\frac{\partial u^{(e)}}{\partial y} \right) + \frac{u^{(e)}}{\lambda^2} \frac{\partial u^{(e)}}{\partial u_i} - \frac{u_\infty}{\lambda^2} \frac{\partial u^{(e)}}{\partial u_i} \right) dA \\ + \iint_A \frac{1}{D_{Ca}} \frac{\partial u^{(e)}}{\partial u_i} \frac{\partial u^{(e)}}{\partial t} dA - \mu^{(e)} \int_{y_i}^{y_j} \frac{\sigma}{D_{Ca}} \frac{\partial u^{(e)}}{\partial u_i} \Big|_{x=-5} dy\end{aligned} \tag{16}$$

Also from (10) we have,

$$\begin{aligned}\frac{\partial u^{(e)}}{\partial x} &= \begin{bmatrix} \frac{\partial N_i}{\partial x} & \frac{\partial N_j}{\partial x} & \frac{\partial N_k}{\partial x} \end{bmatrix} u^{(e)} \\ \frac{\partial}{\partial u_i} \left(\frac{\partial u^{(e)}}{\partial x} \right) &= \frac{\partial N_i}{\partial x} \\ \frac{\partial u^{(e)}}{\partial u_i} &= N_i \\ \frac{\partial u^{(e)}}{\partial t} &= [N] \begin{bmatrix} \frac{\partial u_i}{\partial t} & \frac{\partial u_j}{\partial t} & \frac{\partial u_k}{\partial t} \end{bmatrix}^T\end{aligned} \tag{17}$$

where, $[N] = \begin{bmatrix} N_i & N_j & N_k \end{bmatrix}$. Thus (16) can be written as,

$$\frac{\partial I^{(e)}}{\partial u_i} = K^{(e)}u^{(e)} + M^{(e)}\dot{u}^{(e)} - F^{(e)} = 0 \tag{18}$$

where $\dot{u}$ is used to denote time derivative of 'u' and $K^{(e)}, M^{(e)}, F^{(e)}$ are given by,

$$\begin{aligned} K^{(e)} &= \iint_A \left(\frac{\partial N^{(e)}}{\partial x}\frac{\partial N^{(e)^T}}{\partial x} + \frac{\partial N^{(e)}}{\partial y}\frac{\partial N^{(e)^T}}{\partial y} + \frac{1}{\lambda^2}(N^{(e)}N^{(e)^T}) \right) dA \\ M^{(e)} &= \frac{1}{D_{Ca}} \iint_A N^{(e)}N^{(e)^T} dA \\ F^{(e)} &= \frac{u_\infty}{\lambda^2} \iint_A N^{(e)} dA + \mu^{(e)} \int_{y_i}^{y_j} \frac{\sigma}{D_{Ca}}\, N^{(e)}\big|_{x=-5}\, dy \end{aligned} \tag{19}$$

Further from (11) we have,

$$\begin{aligned} \frac{\partial N_\alpha}{\partial x} &= b_\alpha \\ \frac{\partial N_\alpha}{\partial y} &= c_\alpha \end{aligned} \tag{20}$$

where, $\alpha = i, j, k$. Also, since our triangle is linear by using *factorial formula* we have [10],

$$\begin{aligned} \int\int_A \frac{\partial N^{(e)}}{\partial x}\frac{\partial N^{(e)^T}}{\partial x} dA &= \frac{1}{4A^{(e)}} \begin{bmatrix} b_i^2 & b_ib_j & b_ib_k \\ b_ib_j & b_j^2 & b_kb_j \\ b_ib_k & b_jb_k & b_k^2 \end{bmatrix} \\ \int\int_A \frac{\partial N^{(e)}}{\partial y}\frac{\partial N^{(e)^T}}{\partial y} dA &= \frac{1}{4A^{(e)}} \begin{bmatrix} c_i^2 & c_ic_j & c_ic_k \\ c_ic_j & c_j^2 & c_kc_j \\ c_ic_k & c_jc_k & c_k^2 \end{bmatrix} \\ \int\int_A N^{(e)}N^{(e)^T} dA &= \frac{A^{(e)}}{12} \begin{bmatrix} 2 & 1 & 1 \\ 1 & 2 & 1 \\ 1 & 1 & 2 \end{bmatrix} \\ \int\int_A N^{(e)} dA &= \frac{A^{(e)}}{3} \begin{bmatrix} 1 \\ 1 \\ 1 \end{bmatrix} \end{aligned} \tag{21}$$

For the assembly of all the elements, we write

$$\begin{aligned} K &= \sum_{e=1}^{60} D^{(e)}K^{(e)}D^{(e)^T} \\ M &= \sum_{e=1}^{60} D^{(e)}M^{(e)}D^{(e)^T} \\ F &= \sum_{e=1}^{60} D^{(e)}F^{(e)} \end{aligned} \tag{22}$$

where,

$$D^{(e)} = \begin{bmatrix} 0 & 0 & 0 \\ \vdots & \vdots & \vdots \\ 1 & 0 & 0 \\ 0 & 1 & 0 \\ 0 & 0 & 1 \\ \vdots & \vdots & \vdots \\ 0 & 0 & 0 \end{bmatrix} \begin{matrix} \\ \\ i^{th}row \\ j^{th}row \\ k^{th}row \\ \\ \\ \end{matrix} \tag{23}$$

Thus for the whole system we have,

$$[K]_{37x37}\,[\overline{u}]_{37x1} + [M]_{37x37}\left[\frac{\partial \overline{u}}{\partial t}\right]_{37x1} = [F]_{37x1}$$

References

1. N.L. Allbritton, T. Meyer and L. Stryer, *Range of messenger action of calcium ion and inositol 1,4,5-trisphosphate*. Science, Vol. 258(1992), 1812-1815.
2. K. Broadie, H.J. Bellen, A.Di Antonio, J.T. Littleton and T.L. Schwarz, *Absence of synaptotagmin disrupts excitation-secretion coupling during synaptic transmission*, Proc. Nat. Acad. Sci., Vol. 91(1994), 10727-10731.
3. N. Brose, A.G. Petrenko, T.C. Sudhof and R. Jahn, *Synaptotagmin: a calcium sensor on the synaptic vesicle surface*, Science, Vol. 256(1992), 1021-1025.
4. G.L. Fain, *Moleculer and cellular physiology of neurons*. Prentice Hall of India, 2005.
5. E.R. Kandel, J.H. Schwartz, and T.M. Jessell, *Principles of Neural Science*, 4th ed. McGraw-Hill, New York, 2000.
6. Y.W. Kwon and H. Bang, *The Finite Element Method using MATLAB*, CRC Press, London, 1997.
7. E. Neher, *Concentration profiles of intracellular Ca^{2+} in the presence of diffusible chelator*, Exp. Brain Res. Ser. Vol. 14(1986), 80-96.
8. S.S. Rao, *The Finite Element Method in engineering*, Elsevier Science and Technology books, 2004.
9. S. Rudiger, J.W. Shuai, W. Huisinga, C. Nagaiah, G. Warnecke, I. Parker and M. Falcke, *Hybrid Stochastic and Deterministic Simulations of Calcium Blips*, Biophysical J., Vol. 93(2007), 1847-1857.
10. L.J. Segerlind, *Applied Finite Element Analysis*, John Wiley and Sons, New York, 1984.
11. G.D. Smith, *Analytical Steady-State Solution to the rapid buffering approximation near an open Ca2+ channel*, Biophysical J., Vol. 71(1996), 3064-3072.
12. G.D. Smith, L. Dai, R.M. Miura and A. Sherman, *Asymptotic Analysis of buffered Ca2+ diffusion near a point source*, SIAM J. of Applied of Math., Vol. 61(2000), 1816-1838.
13. G.D. Smith, J. Wagner and J. Keizer, *Validity of the rapid buffering approximation near a point source of Ca2+ ions*, Biophysical J., Vol. 70(1996), 2527-2539.
14. Y. Tang, T. Schlumpberger, T. Kim, M. Lueker, and R.S. Zucker, *Effects of Mobile Buffers on Facilitation: Experimental and Computational Studies*, Biophysical J., Vol. 78(2000), 2735-2751.

Shivendra Gajraj Tewari received his MSc from Jiwaji University, Gwalior and joined as Research Fellow at Maulana Azad National Institute of Technology, Bhopal in 2007. Since, 2007 he is involved in research and has published about 8 papers in international

journals. His research interest focus on Mathematical Modeling of Biological Processes, Computational Neuroscience and Ca^{2+} Dynamics.

Department of Mathematics, Maulana Azad National Institute of Technology, Bhopal 462 051, INDIA.
e-mail: shivendra.tewari@rediffmail.com

Kamal Raj Pardasani recieved his PhD in Mathematics from Jiwaji University, Gwalior in 1988. Presently he is Professor of Mathematics, Bioinformatics, and Computer Applications department at MANIT, Bhopal. He has supervised 10 PhDs and published more than 100 papers in Journals. His current research interests are in the areas of Mathematical and Computational Biology, Computational Neuroscience, Bioinformatics, Biocomputing and Data Mining.

Department of Mathematics, Maulana Azad National Institute of Technology, Bhopal 462 051, INDIA.
e-mail: kamalrajp@rediffmail.com